

## CHAPTER 128

# Physical Experiments on the Effects of Groins on Shore Morphology

Peyman Badiei<sup>1</sup>, J. William Kamphuis<sup>1</sup>, David G. Hamilton<sup>1</sup>

### Abstract

Physical mobile bed models were used to study the morphological effects of groins on an initially straight beach that was exposed to obliquely incident irregular waves. The tests were carried out at two different wave basins with the beach length of 8 and 28 m. A straight beach in the absence of groins was tested for each set of variables, then one or two impermeable surface piercing groins with different lengths were installed and tested. A detailed morphological and hydrodynamic data base was acquired which can be used for calibration and verification of numerical morphology models. Testing procedure and conditions are explained and typical results are presented along with a preliminary analysis which reveals the significant features of the evolution of beach bathymetry.

## 1. Introduction

Mobile bed models are widely used to study the problems dealing with morphological changes of coastal zones. The rapid growth in instrumentation technology has strengthened these models to provide more accurate and reliable results. The application of these models, however, is accompanied by problems associated with scale effects, boundary effects and operational errors discussed among others by Kamphuis (1991) and Hughes (1993). Kraus and Larson (1988) and Larson (1988) discuss examples of the application of large flumes in 2D morphology models to reduce the scale effects. The reduction of scale effects by using large basins, however, is not yet accomplished for a 3D model where wave induced longshore currents play a major role. In spite of these problems, mobile bed models are a unique way of providing a controllable environment for acquiring reliable data and insight into the physical processes.

---

<sup>1</sup> Department of Civil Engineering, Queen's University, Kingston, Ontario, Canada, K7L 3N6

In the present study a series of mobile bed *process models* (Kamphuis (1991)) were employed to investigate the effects of groins on the evolution of shore morphology under the attack of waves approaching with an angle towards the shoreline. These tests were carried out at the Queen's University Coastal Engineering Research Laboratory (QUCERL) and the Hydraulic Laboratory of the National Research Council of Canada (NRCC).

## 2. Objectives

This study attempts to understand the hydrodynamic and sediment processes near groins through the use of both physical and numerical models. The hydraulic model results provide a data base for the calibration and verification of a detailed numerical morphology model. The numerical model in turn will be used first to simulate the hydraulic model results and then to scale up to prototype, thus circumventing some of the shortcomings of the physical model. This paper presents the results of physical experiments.

A review of the very few mobile bed tests on groins reported in the literature (Barcelo (1968) and (1970), Price and Tomlinson (1968) and Hulsbergen et al (1978)) shows that no such comprehensive data base is at hand which can be used for the purpose of this study. The results of the available experiments have some common features; (1) tests were performed with regular waves, (2) they were restricted to one or two aspects and the overall impact of the groins was not investigated and (3) the data collection was limited to recording some parts of the overall process and many important details are lost.

Regular waves have concentrated energy around a single frequency, so they produce exaggerated offshore bar and strong rip currents (described by Hulsbergen et al (1978) as 'chaotic current patterns'). These effects which distort the test results and make the testing operation unmanageable were avoided in the present study by using irregular long crested waves. Moreover irregular waves have a closer resemblance to the waves in prototype. Detailed morphological data were collected along with measurements of hydrodynamic conditions (waves and currents). Because the changes in morphology made it difficult to perform sufficient steady state current measurements, a separate series of fixed bed tests were carried out at QUCERL basin to provide a more detailed hydrodynamic data base. The results of these tests will be discussed in a later paper. Finally, instead of looking at some specific features of morphological changes, within the framework of the variables of these tests (discussed in Section 3), all the important aspects of the groin impact on an initially straight beach were considered. During the tests and in the analysis of the results, special attention was given to the following morphological features:

1. The bar-groin interaction which affects the position of the breaker, the width of the surfzone, the reformation of the longshore current and the sediment transport distribution.

2. The extent and geometry of the accretion and erosion zones on either side of groin(s) which shows the length of the beach affected by the groin. In this regard the accretion and erosion pattern inside the groin bays are also very important.
3. The local scour holes or channels around the groin created by strong currents that are vital to the design of the groin structure.

### 3. Testing Procedure

Among the large number of parameters which could be varied in such tests, it was decided, due to practical limitations, to keep the following parameters constant. Based on a JONSWAP spectrum, irregular wave trains composed of 200 waves with a peak period of  $T_p = 1.15$  s and groupiness factor of  $G = 0.8$  were used. The mean diameter of the sand ( $D_{50}$ ) was 0.12 mm and the initial slope of the beach (m) was 0.1. The deep water wave angle  $\alpha$  and the ratio of  $S_g/L_g$  where  $S_g$  is the distance between the groins and  $L_g$  is the groin length measured from the still water line, were also constants. The variable quantities were the incident wave height  $H_s$ , the position and the number of groins and the ratio of  $L_g/L_b$  where  $L_b$  is the distance of the offshore bar (prior to the installation of any groin) measured from the still water line.

Table 1: QUCERL mobile bed tests summary

Test No.	Test Description	Target $H_s$ (cm)	Duration (hrs)	Estimate $L_g/L_b$	Groin Position (m)
QT1	Single Groin	Variable	---	----	----
QT2	Single Groin	6.0	25.2	1.0	Y = 4.50
QT3	Single Groin	6.0	22.0	0.9	Y = 4.50
QT4	Single Groin	6.0	26.0	1.12	Y = 4.50
QT5	Single Groin	6.0	28.0	0.95	Y = 4.50
QT6	Straight Beach	6.0	24.0	N/A	N/A
QT7	Straight Beach	6.0	24.0	N/A	N/A
QT8	Single Groin	6.0	12.0	0.5	Y = 8.25
QT9	Single Groin	6.0	12.0	1.0	Y = 8.25
QT10	Single Groin	6.0	16.0	1.5	Y = 8.25
QT11	Single Groin	8.0	14.0	1.0	Y = 8.25
QT12	Straight Beach	8.0	12.0	N/A	N/A
QT13	Single Groin	8.0	12.0	0.75	Y = 8.25

Table 2: NRCC mobile bed tests summary

Test No.	Test Description	Target $H_s$ (cm)	Duration (hrs)	Estimate $L_g/L_b$	Groin Position (m)
NT1	Straight Beach	8.0	12.0	N/A	N/A
NT2	Single Groin	8.0	12.0	1.0	Y = 15.50
NT3	Double Groin	8.0	12.0	1.0	Y=18.75 & 15.50
NT4	Double Groin	8.0	12.0	1.4	Y=20.25 & 15.50
NT5	Double Groin	8.0	12.0	0.8	Y=18.10 & 15.50
NT6	Double Groin	10.0	12.0	1.0	Y=20.50 & 15.50
NT7	Double Groin	6.0	12.0	1.0	Y=17.68 & 12.00

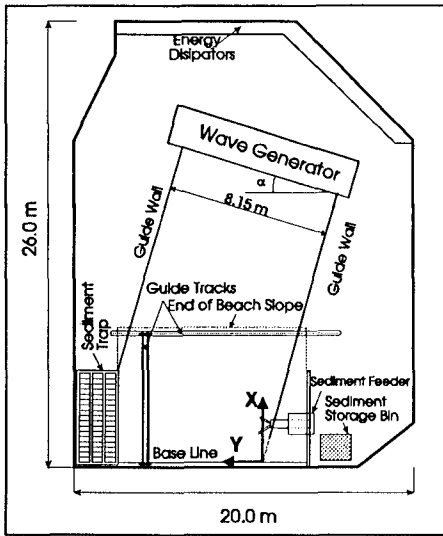


Figure 1: QUCERL Basin

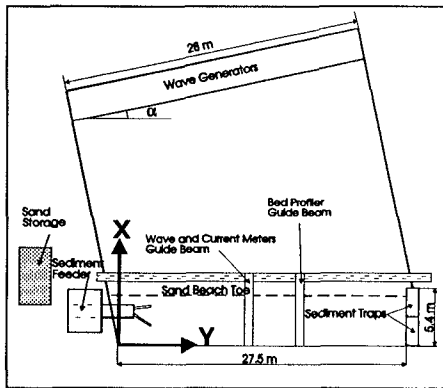


Figure 2: NRCC Basin

Tables (1) and (2) summarize the tests carried out at QUCERL and NRCC respectively. Here  $Y$  is the distance from the updrift wave guide shown in Figures 1 and 2.

At the beginning of each test the sandy beach was reshaped to a plane 1:10 slope. Then the beach was exposed to waves for four hours. At that time a clear offshore bar-trough/step formation (as defined by point 2 in Figure (23)) had developed. When groins were tested they were installed at this stage. The tests were continued thereafter in 2 hour cycles.

Figures 1 and 2 show the layout of the basins at QUCERL and NRCC respectively. Both basins had a closed updrift and an open downdrift boundary and the wave generators were raised above the floor so that water could flow underneath them. This measure according to Kamphuis (1977) would reduce circulation in the testing zone.

For an easier comparison with QUCERL, the NRCC results were transformed into their mirror image so that in all the test results the longshore current flows from right to left.

At QUCERL the angle  $\alpha$  of the wave generator was  $10^\circ$  in a water depth of 0.55 to 0.58 m and at NRCC this angle was  $11.6^\circ$  in a depth of 0.65 m

Wet sediment was fed to the updrift boundary at a rate calculated by the expression developed by Kamphuis (1991a) which yields 27.5, 48 and 74.4 kg/hr of submerged sand for 6, 8 and 10 cm wave heights respectively. This amount was divided into two parts fed separately to the swash zone and near the offshore bar/step. The sediment was trapped at the downdrift boundary and its submerged weight was measured by the loadcells connected to the traps. When the accumulated sand filled the traps it was recirculated into the storage bin near the feeder.

The Generalized Data Analysis Package (GEDAP) developed by NRCC was used for data acquisition. Waves and wave induced currents, submerged weight of the sand in the traps and bottom topography were measured during each two hour testing cycle. Sampling frequency in all these measurements was 20 Hz and sampling duration for waves and currents was 230 s which covered all the 200 waves with an average period of 1.15 s.

Fifteen capacitance type wave probes with 0.20 m spacing measured the wave height profile perpendicular to the shore line from offshore of the breaker up to a point near the still water line. Deep water wave probes (one at QUCERL and three at NRCC) measured the deep water waves.

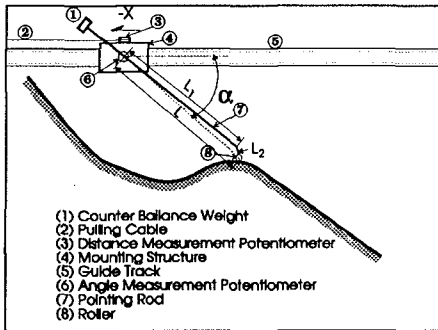


Figure 3: QUCERL Profiler

bed profiler manufactured by Delft Hydraulic Laboratory (Villaneuva(1989)) was used to survey the beach topography. In the other tests another bed profiler, designed and manufactured at QUCERL was used, shown in Figure 3. Here a roller (8) which was connected to the end of a pointing rod (7) followed the beach profile by simply resting on the sand. Knowing the length  $L$  and the angle  $\alpha$  which was measured by the reading of a potentiometer (6), the depth at each point was calculated. The distance in the  $X$  direction from the base line in (shown in Figure 1) was calculated from the readings of another potentiometer (3).

#### 4. Analysis of Morphological Data

The collected data along with the observations while performing the experiments are the basis of this first step of analysis. It should be mentioned that in the contour plots of the bathymetry and wave heights and the velocity vector plots of NRCC test results, the plotted distances in the  $X$  direction appear twice as large as the  $Y$  distances to make the plots clearer. Thus the angles of the velocity vectors are distorted.

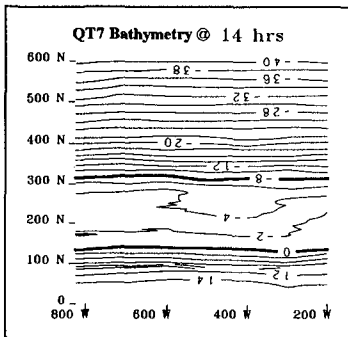
##### 4.1. Straight Beach Tests

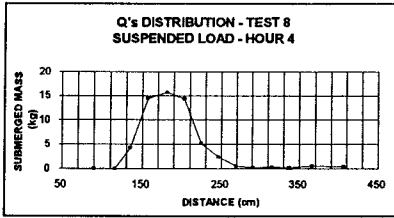
Four straight beach tests without any groins were performed as summarized in Tables 1 and 2. Comparing the results of these tests with the ones performed with

Electromagnetic (EM) bi-directional, sphere-headed current meters were used in both series of tests. Two current meters were used at QUCERL and maximum of four were used at NRCC. They were spaced at a distance greater than 0.25 m to avoid electrical interference. The time averaged velocities in  $X$  and  $Y$  directions were calculated from the measured time series and recorded.

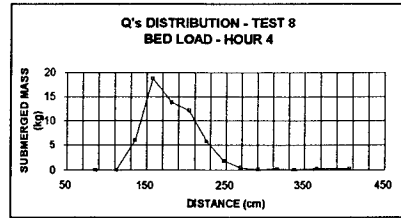
In the first six tests at QUCERL and in all the NRCC tests the PV-07

groins allows the determination of the net effects of the groins. The contour plots of the beach bathymetry for tests QT7 after 14 hours and NT1 after 12 hours of testing are shown in Figures 4 and 5. The straight and parallel contour lines indicate that a straight and long beach was correctly modelled. The averages of three middle profiles (X = 3,4 and 5 m) in QT7 and five middle profiles (X = 13.5, 15.5, 17.5, 19.5 and 21.5 m) in NT1 at different times are shown in Figures 6 and 7. These two Figures suggest that an equilibrium beach profile was not formed even after long hours of testing at QUCERL. They also show that smoother offshore bars were formed compared to the tests with regular waves reported by Larson(1988) and Kamphuis (1994). No build up of the offshore bar was observed after the first four hours of testing as opposed to Larson(1988). The smoother profile of the offshore bar formed by irregular waves is caused by the breaking of individual waves at different locations.

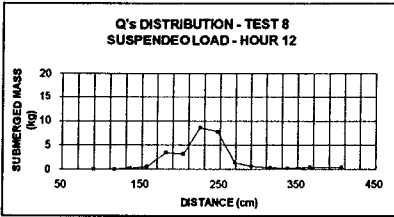




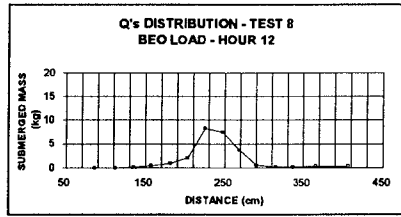
(a)



(b)

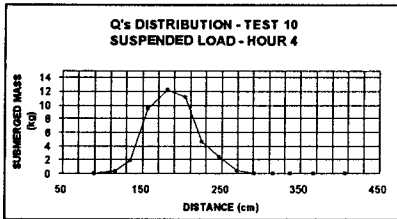


(c)

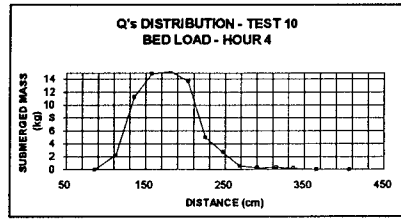


(d)

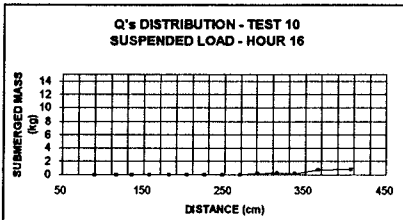
Figure 8: Cross shore sediment transport distribution at 4 and 12 hrs in QT8 with  $L_g/L_b = 0.5$



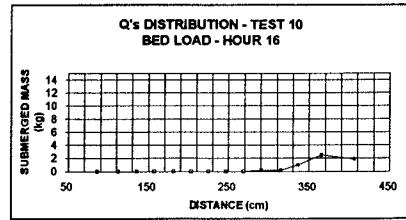
(a)



(b)



(c)



(d)

Figure 9: Cross shore sediment transport distribution at 4 and 16 hrs in QT10 with  $L_g/L_b = 1.5$

distribution of sediment transport rate at the sediment trap are explained in Kamphuis and Kooistra (1990). Figures 8 and 9 show typical examples of these distributions for

two extreme cases of  $L_g/L_b = 0.5$  and  $1.5$  (Tests QT8 and QT10 respectively). These Figures show the distributions at 4 hours with no groin and sometime after the groin was installed. In QT8 a considerable portion of the sand was bypassed into the trap. On the contrary in QT10, after 16 hours, practically no sediment was caught by the trap and all of the sediments were either accreted updrift of the groin or diverted offshore and created a shoal. Figure 8 shows an offshore shift of the peak of the longshore sediment transport rate, indicating that even a short groin deflects the longshore sediment flow.

Figure 10 presents the contours of QT10 at 4 and 16 hours. The still water line called  $L_0$  and the contour line with the closest depth to the breaker depth (here  $-8$  cm) called  $L_{br}$ , are highlighted. These lines are used to trace the evolution of beach bathymetry.  $L_{br}$  and  $L_0$  run almost parallel to each other during this test and both of

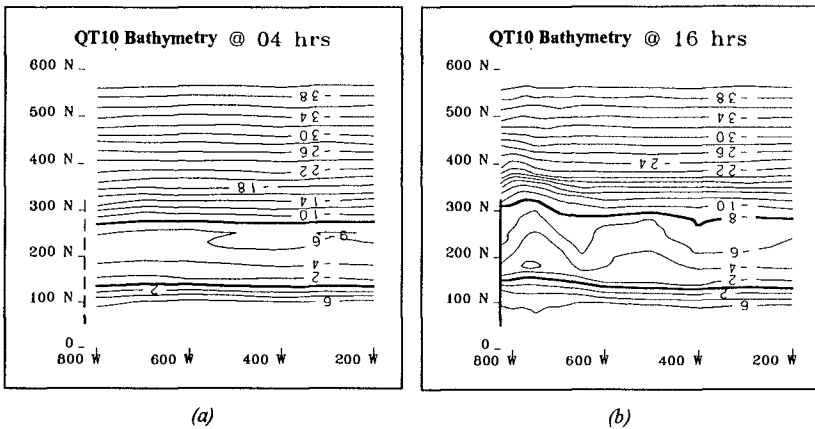


Figure 10:  $H_s = 6$  cm, groin at the sediment trap,  $L_g/L_b = 1.5$ .

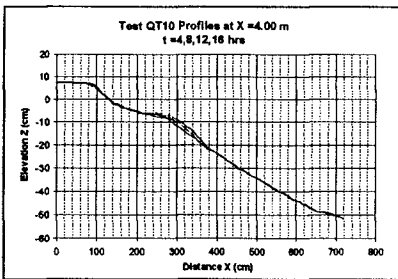


Figure 11: QT10 profiles at  $X=4$  m

them were deflected seaward by the groin.  $L_{br}$ , as shown in Figure 10 almost reached the head of the groin after 16 hrs.

Figure 11 shows that in QT10 the still water line at  $X=4$  m did not recede shoreward. The accretion caused by the groin at this location compensated the recession of the still water line,  $L_0$ , that was observed in the straight beach tests (discussed in Section 4.1). The distance of this point from the groin is almost equal to

that of the updrift boundary from the groin in QUCERL test with a groin in the middle of the basin. Evidently in these tests the groin affects the updrift boundary and the long beach condition updrift of the groin is not valid.

### 4.3. Groin(s) in the Middle of the Basin

#### 4.3.1. Single Groin in the Middle of the Basin

The contour plots of QT3 and NT2 shown in Figures 12 and 13 will be discussed as two examples in this group. Because the boundaries are affected by the groin, the contour pattern on either side of the groin in QT3 does not show the expected shape. Local effects near the groin such as the shift in  $L_0$  on either side of the groin, the deflection of  $L_{br}$  (depth 8 cm) to the offshore direction and the formation of a scour hole near the head of the groin are all well presented by this model, thus the results of this model are still useful as input to a numerical model. Nevertheless, to reduce the boundary effects, similar tests were carried out at NRCC and the result of the test with a single groin is shown in Figure 13 which shows a significant improvement. Here on the updrift side,  $L_0$  remained parallel to its original position far from the groin and advanced seaward close to the groin. Downdrift of the groin  $L_0$  receded shoreward except in the close vicinity of the groin and its direction was similar to that of  $L_0$  on the updrift side. The formation of a scour hole near the head of the groin was also quite obvious. In addition, a shoal was created in front of the groin which was due to the deposition of the deflected longshore sediment flow. Line  $L_{br}$  (depth -10 cm) runs parallel to  $L_0$  on the updrift side and remains parallel to its original alignment downdrift of the groin.

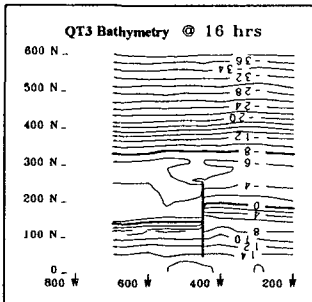


Figure 12:  $H_s = 6$  cm,  $L_g/L_b = 0.9$

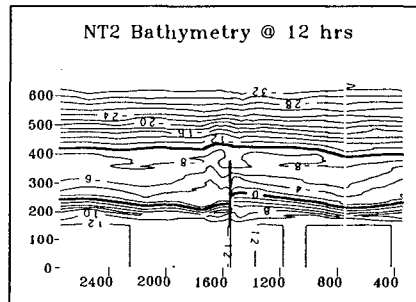


Figure 13:  $H_s = 8$  cm,  $L_g/L_b = 1$ .

#### 4.3.2. Double Groins in the Middle of the Basin

Figures 14-16 show the bathymetry of the tests with double groins with  $L_g/L_b = 0.8$  to 1.4 and  $H_s = 8$  cm at 12 hrs. Note that the updrift sides of Figures 13 and 14 are quite similar which is an indication of the repeatability of the tests. Two distinct shoals were formed offshore of the heads of the groins. These shoals were absent with short groins ( $L_g/L_b = 0.8$ , in test NT5).

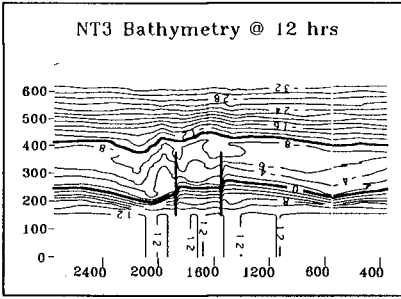


Figure 14:  $H_s = 8$  cm,  $L_g/L_b = 1$ .

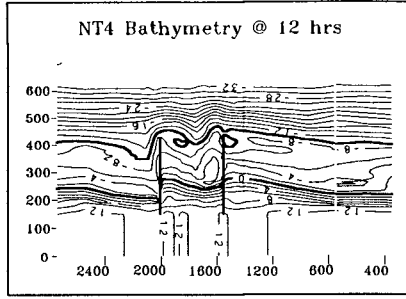


Figure 15:  $H_s = 8$  cm,  $L_g/L_b = 1.4$ .

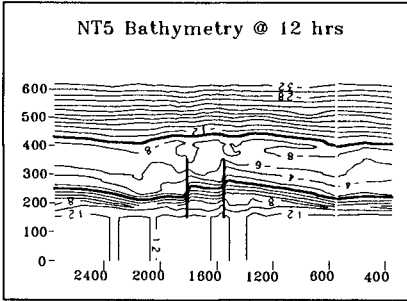


Figure 16:  $H_s = 8$  cm,  $L_g/L_b = 0.8$ .

The bypassed sediments collected down-drift near the groin and partly filled the zone eroded by the sediment transport rate deficit. This formed a depression zone (a ditch) at a distance down-drift of the groin. The ditch was closer to the groin with the longest groin (Figure 15) because the bypassing was small and was almost absent with shortest groin (Figure 16) due to increased bypassing. The contour line pattern on both sides of groins were similar with NT2.

The contour lines in the bay between the groins were more inclined and parallel to the incoming wave crests in NT4 where  $S_g$  was longer and little bypassing into the bay was allowed by the long groin.

Test NT6 with  $H_s = 10$  cm at 12 hrs is shown in Figure 17. The diversion of the more powerful longshore sediment flow caused a distinct offshore shoal, and more offshore contour lines were affected. Finally the topography of the low energy test NT7 at 12 hrs is presented in Figure 18.

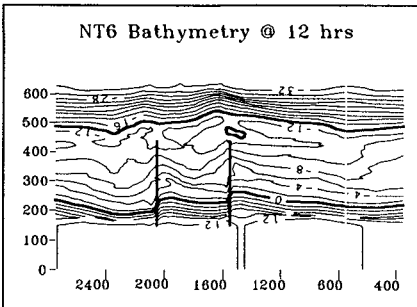


Figure 17:  $H_s = 10$  cm,  $L_g/L_b = 1$ .

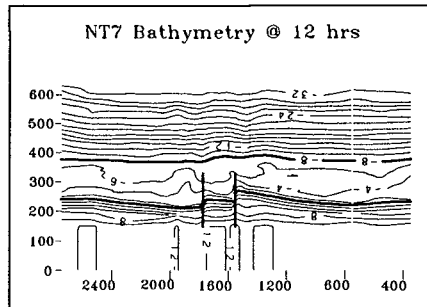


Figure 18:  $H_s = 6$  cm,  $L_g/L_b = 1$ .

In Figures 14-16  $L_{br}$  is the -10 cm contour line. With the short groin shown in Figure 16,  $L_{br}$  is almost unaffected by the groin.  $L_0$  in this case matches the expected pattern. In Figure 14 where  $L_g/L_b=1$ , the groin deflects  $L_{br}$  to some extent and for the case of the long groin shown in Figure 15,  $L_{br}$  is deflected considerably and runs almost parallel to  $L_0$  both updrift and downdrift of the groins. It is seen that the behaviour of  $L_{br}$  depends to a great extent, on the length of the groin.

#### 4.4. Net Morphological Changes Caused by Groins

As shown in Section 4.1 the bottom topographies in all the straight beach tests were continuously evolving and no equilibrium condition was reached. To differentiate between the bottom changes in a straight beach and that caused by the groin(s) the topographies of these two after the same duration of testing were subtracted from each other. Examples are shown in Figures 19-22. Here the dashed contour lines show the eroded zones and the solid lines represent the accreted areas. In all these figures it

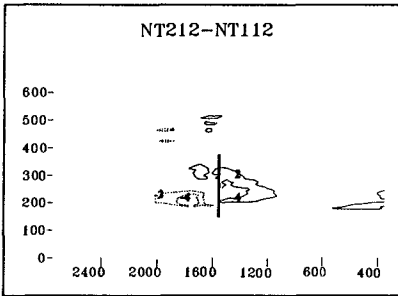


Figure 19: Net groin effect in NT2 at 12 hrs

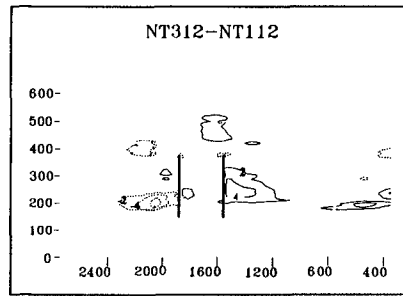


Figure 20: Net groin effect in NT3 at 12 hrs

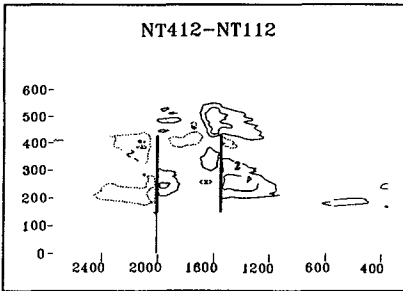


Figure 21: Net groin effect in NT4 at 12 hrs

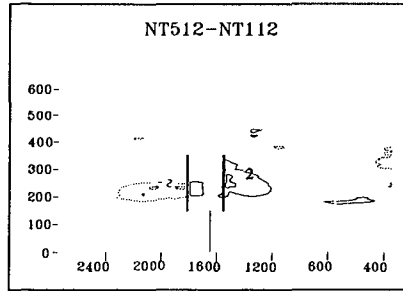


Figure 22: Net groin effect in NT5 at 12 hrs

is seen that the amount of net accretion caused by the groins is considerably more than the net erosion. This is possibly caused by the closeness of the downdrift boundary. It is not far enough from the groin to allow the erosion to compensate the accreted

volume updrift of the groin. The nonuniformity of the longshore current due to the circulation inside the basin could be another reason for this imbalance. The presence of offshore shoal is quite clear in Figures 20 and 21.

#### 4.5. Analysis of Characteristic Lines

The behaviour and evolution of the beach bathymetry can be studied by monitoring the changes in the positions of some *characteristic points* which define the geometry of the active zone of the beach profile. These points are defined in Figure 23. The offshore bar/step position is closely related to the breaker point and the beach head is located at the end of the wave uprush. The beach head and the offshore bar/step also define the boundaries of a *channel* in which most of the longshore sediment flow occurs. A FORTRAN code was written to detect the positions of these points based on the measured profiles.

The results of this analysis on the straight beach in test NT1 is shown in Figure 24. The process of beach profile lengthening in which beach head recedes and bar crest (offshore step) advances offshore is quite apparent if the characteristic lines of this test at different times are compared. It is also seen that the position of the bar crest (or the offshore step) and trough varied along the shore with a maximum difference of about 0.50 m in the X direction. A rip current which pushed the breaker and consequently the offshore bar/step away from the shore line is considered to be the cause of this behaviour. The formation of the rip currents in an experimental wave basin will be presented in more

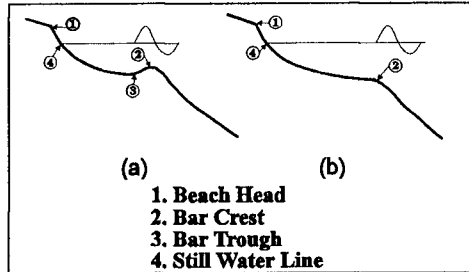


Figure 23: Definition of characteristic points

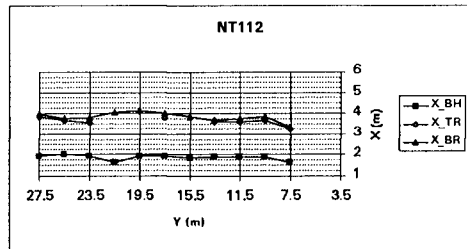


Figure 24: Characteristic lines for NT1 at 12 hrs

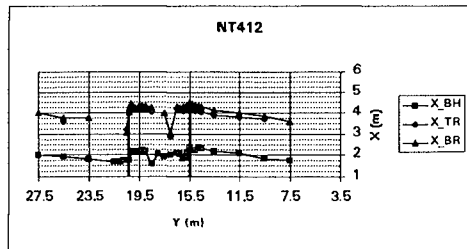


Figure 25: Characteristic lines for NT4 at 12 hrs

detail in a later paper. The comparison of  $L_0$  and  $L_{br}$  in Figure 15 and the bar/step and beach head characteristic lines in Figure 25 shows a similar pattern for the *channel* of longshore current in this test.

## 5. Wave and Current Data

To conduct these tests properly a large number of wave and current measurements within a short period of time were necessary to have a clear impression of waves and current patterns inside the testing zone which is unaffected by the changes in the movable bed. It was decided for practical reasons to perform limited measurements on waves and currents in these series of tests and use a fixed bed model later to acquire more detailed data on waves and currents. At NRCC more data acquisition channels were available, which provided a large number of simultaneous wave measurements. Thus the intensity of wave data within each test cycle was high enough as shown in Figure 26 to give a clear view of the wave pattern around the groins.

Typical results of wave and current measurements are presented in Figure 26 and 27.

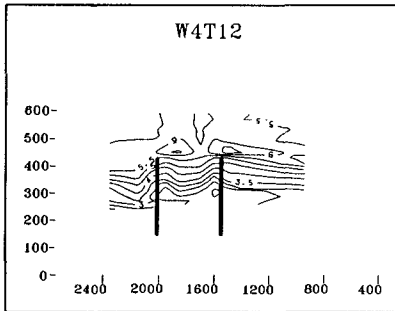


Figure 26:  $H_{ms}$  contours in NT4 at 12 hrs

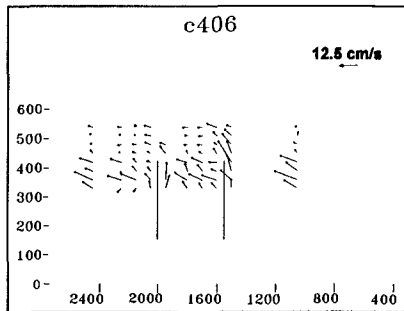


Figure 27: Velocities in NT4 at 6 hrs

## 6. Conclusions:

- Detailed morphological and hydrodynamic data were acquired in a set of mobile bed hydraulic model tests with and without groins
- At QUCERL the short distance of the boundaries from the groin prevented the simulation of a long beach on either side of a groin. The effects of the groin(s) on the boundaries were smaller in the tests at NRCC but not totally eliminated. However the boundary conditions in both series of these tests were measured and knowing these boundary conditions will permit the use of the collected data in a numerical model.

- Straight and parallel contour lines in straight beach tests both at QUCERL and NRCC indicate that a long straight beach was successfully modeled. Equilibrium beach profiles were not observed even after long hours of testing (maximum of 28 hours at QUCERL). In contrast to the tests with regular waves no pronounced offshore bar was formed and in most of the cases an offshore step was created instead of an offshore bar. No build-up of the offshore bar was observed after the first four hours of testing.
- The QUCERL tests with a groin at the trap showed that with a long groin, practically no sand was bypassed into the trap; the sediments were either accreted updrift of the groin or diverted offshore. A short groin on the other hand permitted some bypassing and simply deflected the peak of the longshore sediment transport rate offshore.
- The updrift accretion and downdrift erosion in the NRCC tests were quite similar to the expected pattern formed by groins on a straight and long beach. However, in these tests, the net erosion caused by the groin(s) was less than the net accretion which indicates that the downdrift boundary was not far enough from the groin.
- In the test with two long groins (NT4 ) the span of the bay was long enough and little bypassing was permitted so the contour lines inside the groin bay became parallel with the crests of the incoming waves. For the rest of the tests with double groins, the alignment of the contour lines ( $L_0$  in particular) did not change significantly inside the groin bay.
- The bypassing of sand created a shoal offshore of the head of the groin. The size of the shoal was proportional to the length of the groin. Longer groins diverted more sand offshore and created a more distinct shoal.
- The formation of a depression zone downdrift of the groin was also caused by sand bypassing. The depression zone which had the form of a ditch or a channel, was aligned with an angle to the groin and its location was farther from the groin when the groin was shorter. In prototype such a ditch will not be formed because of the variations in the wave condition. But its presence in these experiments with a persistent wave condition is essential to test the ability of a detailed numerical model to correctly simulate this process.
- The formation of a scour hole near the head of the groin is quite evident in all the tests both at QUCERL and at NRCC. The scouring channels however are not shown in the bathymetry plots because of the resolution of the surveying.
- The presence of rip currents in the NRCC basin was shown by the analysis of characteristic lines. Rip currents pushed the location of the breaker point and consequently the offshore bar/step away from the shore and caused changes in the position of characteristic points i.e. offshore bar/step, along the shore of a beach without groins.

## 7. References:

- Barcelo' J.P. (1968)**, "Experimental Study of the Hydraulic Behavior of Groyne System", Proc. 11th Coastal Eng. Conf. pp 326-548
- Barcelo' J.P. (1970)**, "Experimental Study of the Hydraulic Behavior of Inclined Groyne System", Proc. 12th Coastal Eng. Conf. pp 1020-1040
- Hughes S.A. (1993)**, "Physical Models and Laboratory Techniques in Coastal Engineering", Advanced Series on Ocean Engineering - Vol. 7, World Scientific Publishing.
- Hulshergen C.H., Bakker W.T., and Van Bochove G. (1976)**, "Experimental Verification of Groyne Theory", Proc. 15th Coastal Eng. Conf. pp 322-335
- Kamphuis J.W. (1977)**, Discussion on "Wave-Induced Circulation in Shallow Basins" By: Dalrymple R.A., Eubanks R.A., and Birkemeier W.A. (1977), J. of the Waterway , Port, Coastal and Ocean Eng., ASCE, Vol. 103, No. WW1, pp 570-571.
- Kamphuis J.W. and Kooistra J (1990)**, "Three Dimensional Mobile Bed Hydraulic Model Studies of Wave Breaking Circulation and Sediment Transport Processes", Proc. of Canadian Coastal Conference, Kingston, National Research Council of Canada, pp 363-386.
- Kamphuis J.W. (1991)**, "Physical Modelling", Chapter 21, Vol. 2, Handbook of Coastal and Ocean Engineering, Gulf Publishing.
- Kamphuis J.W. (1991a)**, "Alongshore Sediment Transport Rate", J. of Waterways , Ports, Coastal and Ocean Eng., ASCE, Vol. 117, No. 6, pp 624-640.
- Kamphuis J.W. (1995)**, "Comparison of Two-Dimensional and Three-Dimensional Beach Profiles" ,to be published in May 1995, J. of the Waterway , Port, Coastal and Ocean Eng., ASCE.
- Kraus N.C. and Larson M. (1988)**, "Beach Profile Change Measured in the Tank for Large Waves, 1956-1957 and 1962", Technical Report CERC-88-00, Coastal Engineering Research Center, U.S. Army Engineer Waterways Experimental Station, Vicksburg, MS.
- Larson M. (1988)**, "Quantification of Beach Profile Change", Department of Water Resources Engineering, Lund University of Science and Technology, Report No. 1008
- Price W.A. and Tomlinson K.W. (1968)**, "The Effect of Groynes on Stable Beaches", Proc. of 11th Coastal Eng. Conf. pp 518-525
- Villanueva, L.F. (1989)**, "A Novel Technique of Automatic Beach Profile Measurements", Proc. Workshop on Instrumentation, Burlington, Ontario, Canada